

Observation of five additional thermal donor species TD12 to TD16 and of regrowth of thermal donors at initial stages of the new oxygen donor formation in Czochralski-grown silicon

W. Götz and G. Pensl

*Institut für Angewandte Physik, Universität Erlangen-Nürnberg,
Staudtstrasse 7, W-8520 Erlangen, Federal Republic of Germany*

W. Zulehner

Wacker-Chemitronic, P.O. Box 1140, W-8263 Burghausen, Federal Republic of Germany

(Received 28 May 1992)

Thermal donors (TDs) are generated in Czochralski-grown silicon by heat treatments at temperatures around 470 °C. They form a family of individual species with differing ionization energies and act as double donors (TDx^0 , TDx^+). Up to 11 species are already known. We have identified five further effective-mass-like TD species termed TD12 to TD16. Subsequent annealing at 620 °C for 30 min reduces the generated TDs by at least 2 orders of magnitude. With increasing annealing time (30–180 min), an intermediate regrowth of species TD1 to TD4 is observed in parallel with the initial formation of the so-called new oxygen donors.

INTRODUCTION

Czochralski (CZ)-grown silicon contains oxygen concentrations up to $2 \times 10^{18} \text{ cm}^{-3}$ corresponding to the solubility of oxygen at the melting point of silicon. The isolated oxygen atoms are arranged in a puckered $Si_s-O_i-Si_s$ configuration displaced off the $\langle 111 \rangle$ axis at an interstitial site.¹ There the oxygen atoms are electrically inactive but give rise to several IR-active vibrational modes.^{2,3} At elevated temperatures oxygen becomes mobile in the silicon lattice. During heat treatments, oxygen forms clusters or precipitates which apparently act as donors.

Thermal donors (TDs) and new oxygen donors (NDs) are generated in the temperature ranges of 350–500 °C and 550–800 °C, respectively.^{4–10} Although intensive research has been conducted on oxygen-rich silicon since the middle of the 1950s,^{11,12} the chemical nature and the atomic structure of oxygen-related donors are not understood yet. A series of TD models is proposed (e.g., see reviews in Refs. 13–16), but none of these models can consistently explain all the experimental details that are available for oxygen-related donors.

TDs act as double donors. Eleven individual neutral TDx^0 ($x=1-11$) and nine singly charged TDx^+ ($x=1-9$) species have been observed in IR spectra.⁷ The individual TDx^0 and TDx^+ species have slightly differing ionization energies ranging from 69.2 to 49.9 meV and from 156.3 to 116.0 meV, respectively. In contrast to the thermal donors, NDs have a continuous distribution of trap states with respect to energy in the band gap of Si.¹⁰

In the present paper, the individual TDx^0 species are studied by IR absorption. We observed five new effective-mass-like TDx^0 ($x=12-16$) species. In addition, we demonstrate that an intermediate regrowth of TD1 to TD4 species occurs at initial stages of the ND formation.^{17,18}

EXPERIMENTAL DETAILS

We employed selected CZ-grown silicon wafers of (100) orientation supplied by Wacker Chemitronic. The wafers are phosphorus-doped ($\rho=192 \text{ } \Omega \text{ cm}$); the content of oxygen and carbon are $[O_i]=1.27 \times 10^{18} \text{ cm}^{-3}$ and $[C_s] < 5 \times 10^{15} \text{ cm}^{-3}$, respectively. Both faces of the wafers are optically polished, the wafer thickness is 2.5 mm. For the investigations, we used square-shaped samples of $10 \times 10 \text{ mm}^2$ size. Heat treatments are performed in a rapid isothermal annealing (RIA) system under vacuum conditions ($p=10^{-5} \text{ Torr}$). The RIA system used provides 12 tungsten lamps with an electrical power of 12 kW. The temperature is measured with a special sensor consisting of a W/Re thermocouple molten in a Si plate of appropriate size and surface preparation. The total donor concentration is obtained from an analysis of the resistivity, which is measured at room temperature by the four-point-probe method.¹⁹ The conversion of resistivity into TD concentration is based on the assumptions that TDs are double donors, TDs are completely ionized, and the mobility of free electrons is not affected by TDs. The content of individual TDx species and of interstitial oxygen are detected by IR absorption. The IR spectra are taken with a FTIR Nicolet 740 system; the employed resolution is 1 cm^{-1} . The evaluation of TDx concentrations is based on optical cross sections given by Ref. 20. The vibrational mode at $\tilde{\nu}=1127 \text{ cm}^{-1}$ is monitored at 78 K to determine the interstitial oxygen concentration; the calibration factor used is according to the Deutsches Institut für Normung standard.²¹

EXPERIMENTAL RESULTS AND DISCUSSION

Heat treatments of the starting Si material at 470 °C for 3 h result in a total TD concentration of $5 \times 10^{15} \text{ cm}^{-3}$

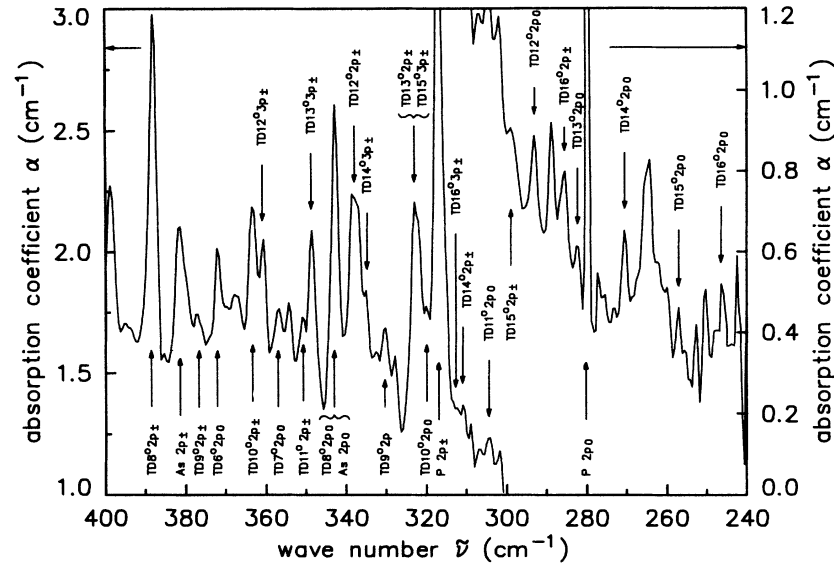


FIG. 1. Absorption spectrum of different TDx^0 species ($x = 6-16$) in phosphorous-doped CZ-grown Si material taken after a heat treatment at 470°C for 3 h.

and in an $[O_i]$ reduction of $\sim 5\%$. IR spectra of TDs are taken at 9 K. At that temperature, the Fermi level is located 27 meV below the conduction band edge indicating that all TDs are in the neutral state. Figure 1 shows a typical absorption spectrum of the heat treated Si samples; the wave numbers range from 400 to 240 cm^{-1} . The high-energy part of the spectrum ($400-300\text{ cm}^{-1}$) is re-

TABLE I. IR absorption line positions $\tilde{\nu}$ and experimental binding energies E_B of $TD12^0$ to $TD16^0$ species are listed in columns 2-5. For comparison, binding energies of an effective-mass-like, hydrogenic defect center calculated after Faulkner (Ref. 22) are given in the last column.

$\tilde{\nu}$ (cm^{-1})						
E_B (meV)	TD12	TD13	TD14	TD15	TD16	EMA
$\tilde{\nu}$ ($5p_{\pm}$)	378	363	350	339	327	
E_B	1.49	1.61	1.61	1.36	1.35	1.44
$\tilde{\nu}$ ($4p_{\pm}$)	372	358	346	332	(320)	
E_B	2.23	2.23	2.36	2.22		2.19
$\tilde{\nu}$ ($3p_{\pm}$)	362	349	335	323	312	
E_B	3.46	3.34	3.46	3.33	3.21	3.12
$\tilde{\nu}$ ($3p_0$)	346	331	319	305	292	
E_B	5.45	5.57	5.45	5.57	5.69	5.48
$\tilde{\nu}$ ($2p_{\pm}$)	338	324	311	298	286	
E_B	6.40	6.40	6.40	6.40	6.40	6.40
$\tilde{\nu}$ ($2p_0$)	293	282	270	259	247	
E_B	12.0	11.7	11.5	11.3	11.3	11.5
$E_B(\text{gs})$	48.3	46.6	45.0	43.4	41.9	31.3

lated to the left y scale, while the low-energy range ($310-240\text{ cm}^{-1}$) is related to the right y scale. The absorption coefficient is determined by considering multiple reflection and a reflection coefficient of 0.3. The observed spectrum is identified as a superposition of absorption lines belonging to transitions from the ground state to bound states ($2p_0, 2p_{\pm}, 3p_0, \dots$) of different TDx^0 species ($TD6^0$ to $TD16^0$). The lines in Fig. 1 are partially marked by the number of the TDx^0 species and by the final state of the transition (e.g., $TD16^0 2p_0$). We also observed absorption lines in the wave-number range from 550 to 400 cm^{-1} (not shown in Fig. 1) which can be largely attributed to $TD1^0$ to $TD7^0$ species.⁸ Singly ionized TDx^+ species cannot be detected because the investigated samples are not highly compensated. Absorption lines of $TD1^0$ to $TD11^0$ species are already described by several authors,⁵⁻⁸ however, the line pattern belonging to $TD12^0$ to $TD16^0$ is reported for the first time. It is assumed that these donors develop from lower numbered TDx species by adding additional atoms (e.g., oxygen atoms or silicon interstitials). This mechanism may lead to a spatial enlargement of TD centers and hence to a greater delocalization of the electron wave function. Absorption lines ($TD12^0$ to $TD16^0$) belonging to these new TD species are summarized in Table I together with the experimentally determined binding energies. In the last column, binding energies of an effective-mass-like, hydrogenic defect center are listed. These values are calculated according to the effective mass approximation (EMA) after Faulkner²² taking into account an anisotropy of effective electron masses of $m_{\perp}/m_{\parallel}=0.2079$. The experimental binding energies are obtained by assuming that the binding energy of $2p_{\pm}$ states is equal to the EMA value of 6.40 meV for all TDx^0 species under consideration. The experimental binding energies of excited states fit well to the corresponding calculated EMA values confirming that TDx^0 centers ($x=12-16$) are EMA-like defect centers. A comparison of the ground-state energies

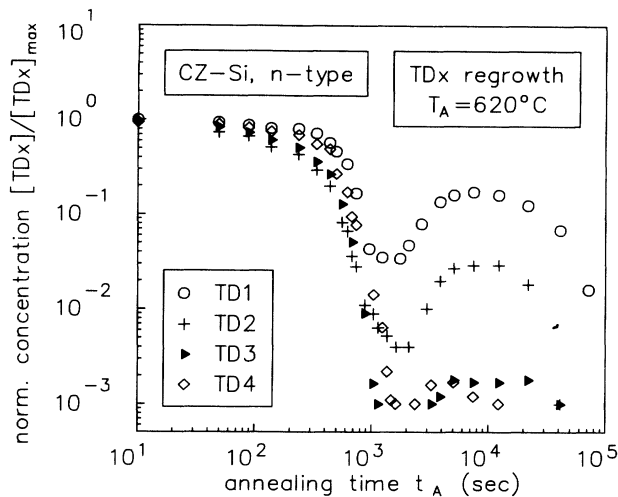


FIG. 2. Individual normalized concentrations $[TDx]/[TDx]_{\max}$ ($x=1-4$) as a function of annealing time t_A recorded for an annealing temperature of 620°C . The thermal history of the investigated samples is discussed in the text.

reveals larger differences which may be attributed to incomplete screening of the core by the second electron of the double donor.⁸ The experimental binding energies of TDx^0 ($x=12-16$) ground states $E_B(\text{gs})$ successively decrease with increasing number x . Their values smoothly continue the binding energies⁸ of $TD1^0$ to $TD11^0$ species and are clearly different from the shallow thermal donors detected by Navarro *et al.*²³ Nearly the complete spectrum in Fig. 1 can be assigned to electronic transitions of effective-mass-like centers. TDx^0 species with $x > 16$ are not identified in the absorption pattern. An extension of the spectrum to smaller wave numbers ($\tilde{\nu} < 240 \text{ cm}^{-1}$) is not feasible with the IR spectrometer used because of its strong decrease in sensitivity in this wave-number range.

The Si samples are exposed to further heat treatments at temperatures between 565 and 620°C for differing annealing times to study the annihilation kinetics of individual TDx species.^{17,24} Generally all individual TDx species are annihilated at 620°C , however, in the following investigation, we consider only the first four TDx species, for which we observed a regrowth in parallel with initial formation of new oxygen donors. In Fig. 2, it is demonstrated that the starting concentrations $[TDx]_{\max}$ of the considered TDx centers are reduced to a minimum value $[TDx]_{\min}$ after approximately 30 min. This annealing process is accompanied by a decrease of the free-electron concentration by almost 3 orders of magnitude and by an increase of $[O_i]$ which reaches again the starting value. The O_i regeneration is supposed to be due to the release of oxygen atoms from oxygen clusters which are dissolved at the temperatures employed. The onset of the decay of $TD1^0$ occurs after the other three TDx^0 species were already partially annihilated; then the decrease of the $TD1^0$ concentration develops rapidly. The annealing behavior of $TD1$ is discussed in Ref. 24. With increasing annealing time ($t_A > 40$ min) a regrowth of

TABLE II. Individual TDx concentrations ($x=1-6$) after different heat treatments are summarized in columns 2-4; the annealing parameters employed are indicated in the corresponding columns. The detection limit is represented by dl.

TD species	Growth (3 h)	Annihilation	Regrowth
	$T_A = 470^\circ\text{C}$	$T_A = 565-620^\circ\text{C}$	$T_A = 620^\circ\text{C}$
	$[TDx]_{\max}$ (cm^{-3})	$[TDx]_{\min}$ (cm^{-3})	$[TDx]_{R,\max}$ (cm^{-3})
1	1.3×10^{14}	4.3×10^{12}	1.3×10^{13}
2	2.0×10^{14}	0.8×10^{12}	5.6×10^{12}
3	3.1×10^{14}	0.1×10^{12}	0.6×10^{12}
4	3.0×10^{14}	0.2×10^{12}	0.5×10^{12}
5	1.5×10^{14}	< dl	< dl
6	0.4×10^{14}	< dl	< dl

TDx^0 species ($x=1-4$) is observed, reaching a new maximum concentration $[TDx]_{R,\max}$ after approximately 2 h. Such a regrowth cannot be observed within the detection limit of 10^{11} cm^{-3} for TDx species with $x \geq 5$. The concentrations of the first four TDx^0 species decrease again with further increasing annealing time. The values of $[TDx]_{\max}$, $[TDx]_{\min}$, and $[TDx]_{R,\max}$ are summarized in Table II. The regrowth of TD centers is accompanied by a strong decrease of interstitial oxygen (up to 80%) and by a renewed increase of free electrons which are now caused by the formation of NDs. The ND activation is proposed to originate from interface states at the surface of SiO_y precipitates.¹⁰

As shown in Fig. 2, the formation of TDx^0 species ($x=1-4$) is also promoted at elevated temperatures. However, at those temperatures, there are several competitive processes like the highly O_i -consuming ND formation or the dissolution of instable small nucleation seeds preventing possibly a continuous regrowth of TDx species. A comparison of the distributions of residual TDx concentrations $[TDx]_{\min}$ ($x=1-6$) and of the regrown maximum concentrations $[TDx]_{R,\max}$ after prolonged annealing at 620°C clearly indicates that the observed increase of TDx^0 species ($x=1-4$) is not caused by back formation of higher numbered TDx complexes but by the renewed growth of these particular TDx species.

In summary, we demonstrate the existence of five new effective-mass-like TDx species ($x=12-16$). They are supposed to develop from the known TDx species ($x=1-11$) by adding additional atoms. The chemical nature of these atoms is not identified yet but it is argued that oxygen plays an important role for the TD formation mechanism. We documented further the intermediate regrowth of $TD1$ to $TD4$ species at initial stages of ND formation at 620°C .

ACKNOWLEDGMENTS

The authors are grateful to Dr. P. Wagner, Wacker-Chemitronic, for helpful discussions.

- ¹J. W. Corbett, R. S. McDonald, and G. D. Watkins, *J. Phys. Chem. Solids* **25**, 873 (1964).
- ²K. Graaff, E. Grallath, S. Ades, G. Goldbach, and J. Toelg, *Solid State Electron.* **16**, 887 (1973).
- ³P. Wagner, *Appl. Phys. A* **53**, 20 (1991).
- ⁴A. Kanamori and M. Kanamori, *J. Appl. Phys.* **50**, 8095 (1979).
- ⁵D. Wruck and P. Gaworzewski, *Phys. Status Solidi (a)* **56**, 577 (1979).
- ⁶F. F. Schaake, S. C. Barber, and R. F. Pinizotto, in *Semiconductor Silicon 1981*, edited by H. R. Huff, R. J. Kriegler, and Y. Takeishi (The Electrochemical Society, Inc., Pennington, NJ, 1981), p. 273.
- ⁷B. Pajot, H. Compain, J. Lerouille, and B. Clerjaud, *Physica* **117 & 118B**, 110 (1983).
- ⁸P. Wagner and J. Hage, *Appl. Phys. A* **49**, 123 (1989).
- ⁹P. Capper, A. W. Jones, E. J. Wallhouse, and J. G. Wilkes, *J. Appl. Phys.* **48**, 1646 (1977).
- ¹⁰G. Pensl, M. Schulz, K. Hölzlein, W. Bergholz, and J. L. Hutchison, *Appl. Phys. A* **48**, 49 (1989).
- ¹¹C. S. Fuller, J. A. Ditzenberger, N. B. Hannay, and E. Buehler, *Phys. Rev.* **96**, 833 (1954).
- ¹²W. Kaiser, H. L. Frisch, and H. Reiss, *Phys. Rev.* **112**, 1546 (1958).
- ¹³G. S. Oehrlein and J. W. Corbett, *Mater. Res. Soc. Symp. Proc.* **14**, 107 (1983).
- ¹⁴P. Wagner, C. Holm, E. Sirtl, R. Oeder, and W. Zulehner, in *Festkörperprobleme (Advances in Solid State Physics)*, edited by P. Grosse (Vieweg, Braunschweig, 1984), Vol. XXIV, p. 191.
- ¹⁵G. Pensl, in *Physical Problems in Microelectronics*, edited by J. Kassabov (World Scientific, Singapore, 1987), p. 155.
- ¹⁶P. Déak, M. Heinrich, L. C. Snyder, and J. W. Corbett, *Mater. Sci. Forum* **83-87**, 395 (1992).
- ¹⁷W. Götz and G. Pensl, *Verh. Dtsch. Phys. Ges. (VI)* **26**, 1187 (1991).
- ¹⁸B. A. Andreev, V. G. Golubev, V. V. Emtsev, G. I. Kroptov, G. A. Oganessian, and K. Schmalz, *Pis'ma Zh. Eksp. Teor. Fiz.* **55**, 52 (1992) [*JETP Lett.* **55**, 52 (1992)].
- ¹⁹See Deutsches Institut für Normung, Standard No. 50431.
- ²⁰P. Wagner, *Mater. Res. Soc. Symp. Proc.* **59**, 125 (1986).
- ²¹See Deutsches Institut für Normung, Standard No. 50348.
- ²²R. A. Faulkner, *Phys. Rev.* **184**, 713 (1969).
- ²³H. Navarro, J. Griffin, J. Weber, and L. Genzel, *Solid State Commun.* **58**, 151 (1986).
- ²⁴W. Götz and G. Pensl (unpublished).